

## Electron affinity of indium and the fine structure of $\text{In}^-$ measured using infrared photodetachment threshold spectroscopy

C. W. Walter,<sup>\*</sup> N. D. Gibson,<sup>†</sup> D. J. Carman, Y.-G. Li (李伊格), and D. J. Matyas  
*Department of Physics and Astronomy, Denison University, Granville, Ohio 43023, USA*

(Received 24 June 2010; published 17 September 2010)

Binding energies of the fine-structure levels of the indium negative ion  $\text{In}^-$  are measured using infrared photodetachment threshold spectroscopy. The relative cross section for neutral atom production is measured with a crossed ion-beam–laser-beam apparatus over selected photon energy ranges between 300 and 700 meV. An  $s$ -wave threshold is observed due to the opening of the  $\text{In}^- (5p^2\ ^3P_0)$  to  $\text{In}(5p\ ^2P_{1/2})$  ground-state-to-ground-state transition, which determines the electron affinity of In to be 383.92(6) meV. The present result is in good agreement with previous theoretical calculations, but it differs substantially from the previously measured electron affinity and reduces the uncertainty by a factor of 150.  $s$ -wave thresholds are also observed for detachment from the excited fine-structure levels of  $\text{In}^-$ , permitting accurate determination of the fine-structure intervals of 76.06(7) meV for  $J = 0-1$  and 170.6(6) meV for  $J = 0-2$ , which are in good agreement with the previous measurements and substantially reduce the uncertainties.

DOI: [10.1103/PhysRevA.82.032507](https://doi.org/10.1103/PhysRevA.82.032507)

PACS number(s): 32.10.Hq, 32.80.Gc

Negative ions are of interest for both applied and fundamental reasons [1]. They are important in a variety of physical situations, ranging from plasmas and discharges to atmospheric chemistry. Since the extra electron in a negative ion is not bound by a net Coulomb field, electron correlation is a dominant factor in their structure and stability. Thus studies of negative ions yield key insights into the dynamics of multielectron interactions, serve as important tests of detailed atomic structure calculations, and provide a valuable opportunity to investigate the general problem of many-body interactions.

The development of new tunable, narrow-bandwidth light sources in the infrared over the past 10–15 years, coupled with more standard visible and ultraviolet lasers, has made it possible to reach the thresholds for photodetachment for most elements that form stable negative ions. This advance has triggered a large number of experimental investigations [2–8], but some atomic electron affinities and negative-ion fine-structure splittings are still not known to a high precision (sub-meV uncertainty) [9–11]. All elements in group III (B, Al, Ga, In, and Tl) form stable negative ions with binding energies of less than 0.5 eV [9], requiring midinfrared light to photodetach at the ground-state threshold. High-resolution threshold spectroscopy has been performed on the lightest two members of the group ( $\text{B}^-$  [2] and  $\text{Al}^-$  [3]) using Raman-shifted light from a dye laser, but the heavier members of group III have not previously been investigated with threshold spectroscopy [12]. In the present study, photodetachment threshold spectroscopy with a narrow-bandwidth tunable infrared optical parametric oscillator-amplifier (OPO-OPA) was used to determine the electron affinity of In and the fine-structure energy intervals of  $\text{In}^-$  with sub-meV uncertainty.

The ground-state valence configuration of neutral In is  $5p^2P_{1/2}$ , with the excited fine-structure level  $^2P_{3/2}$  lying higher

in energy by 274.3272 meV [13] (throughout this paper, the conversion factor  $1\text{ meV} = 8.065\,544\,65\text{ cm}^{-1}$  from CODATA 2006 [14] is used). The configuration of the negative ion  $\text{In}^-$  is  $5p^2\ ^3P_{0,1,2}$ , with the lowest energy level being  $J = 0$  (see energy level diagram in Fig. 1). The first detailed experimental investigation of  $\text{In}^-$  was performed by Williams *et al.* [15] using fixed-frequency laser photodetachment electron spectroscopy. That study yielded 404(9) meV for the electron affinity of In and fine-structure intervals for  $\text{In}^-$  of 76(9) meV for  $J = 0-1$  and 175(9) meV for  $J = 0-2$ .

At least six theoretical studies of  $\text{In}^-$  have been reported [16–21] using a variety of calculational methods that yielded electron affinities ranging between 371 and 419 meV (see Table II for a summary of theoretical results).  $\text{In}^-$  presents a challenge for theoretical analysis because it has a quasidegenerate energy spectrum created by a few relatively strongly correlated configurations; therefore, it is very important to use a multireference approach for a qualitatively correct description of the negative ion spectrum [22]. Furthermore, the core-correlation effects are significant but difficult to predict, since core-valence interactions may make either a net positive or a net negative contribution to the electron affinity. For indium, core correlation appears to lead to a destabilization of the negative ion relative to the neutral atom because the more diffuse valence shell in the negative ion overlaps less with the core electrons [20].

In the present investigation, laser photodetachment threshold spectroscopy has been used to precisely measure the binding energies of each of the three fine-structure levels of  $\text{In}^-$ . The relative cross section for photodetachment from negative ions was measured as a function of photon energy using a crossed ion-beam–laser-beam system. Much of this experimental system has been described in detail elsewhere [7,8]; the main difference from our previous studies is that a new laser system was used in the present experiments. The new laser system is tunable much farther into the infrared (up to 5000 nm) than our previous system (up to 2500 nm), which was necessary to reach the low-energy ground-state thresholds in the present study. In addition, the new laser

<sup>\*</sup>walter@denison.edu

<sup>†</sup>gibson@denison.edu

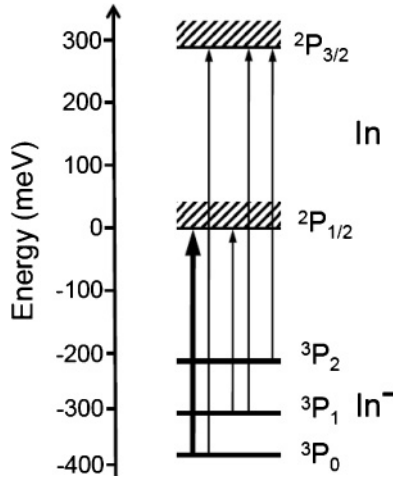


FIG. 1. Energy level diagram for the fine-structure levels of the  $5p^2\ ^3P$  state of  $\text{In}^-$  and the  $5p^2\ ^2P$  state of  $\text{In}$ . The energies of the  $\text{In}^-$  states are based on the present measurements and the energy of the  $\text{In}$   $J = 3/2$  state is from Ref. [13]. Thresholds measured in the present study are shown by vertical arrows, with the electron affinity defining threshold ( $^3P_0 \rightarrow ^2P_{1/2}$ ) in boldface.

system permits continuous scanning of the wavelength and it was used together with a new data acquisition method that recorded information for each individual laser pulse, in contrast to our previous method, in which the wavelength was moved in fixed wavelength steps and only average data for multiple shots were recorded. Negative ions were produced by a cesium sputtering source (NEC SNICS II) using a cathode packed with a solid indium plug. Ions were accelerated to 12 keV and the  $^{115}\text{In}^-$  isotope was mass selected using a  $90^\circ$  focusing sector magnet. Sets of electrostatic lenses and deflection plates both before and after the magnet were used to collimate and steer the beam into a UHV interaction chamber. Beam profile monitors situated both before and after the magnet provided real-time information on the ion beam shape and position. In the interaction region, the ion beam was intersected perpendicularly by a pulsed laser beam. Following the interaction region, residual negative ions in the beam were electrostatically deflected into a Faraday cup to monitor the ion current. Typical ion beam currents of  $^{115}\text{In}^-$  were  $\sim 0.1$  nA. Neutral atoms continued undeflected to strike a multidynode electron multiplier detector. The production of neutral atoms by stripping collisions with background gas was low due to the UHV pressure in the interaction chamber ( $\sim 5 \times 10^{-10}$  Torr) and was accounted for in the analysis, as described here.

The detector was operated in analog mode and the voltage output was recorded as a function of time after each laser pulse using a digital storage oscilloscope. The oscilloscope functioned effectively as a time-gated integrator: the detector voltage was integrated over the arrival window corresponding to the flight time of photodetached neutral  $\text{In}$  atoms from the interaction region to the detector. The background voltage was subtracted from this integrated voltage to obtain a signal proportional to the number of neutral atoms produced by each laser pulse. A LABVIEW computer program was used to interface with the oscilloscope and record the ion beam current, the measured wavelength, and the laser pulse energy

for each shot. The neutral atom signal was then normalized to the ion beam current and the laser photon flux to obtain the relative cross section for photodetachment. Spectra were built up by repeatedly scanning the laser wavelength over the range of interest in continuous scans at rates of up to 0.05 nm/s, then sorting the data into photon energy bins of selectable width. For each spectrum, 10 or more sweeps were combined to give several hundred to several thousand laser shots per bin. Careful tests of the linearity of the overall system were made to ensure that saturation effects were not significant under the experimental conditions used to measure the spectra. The laser system consisted of a tunable OPO-OPA (LaserVision) pumped by a pulsed Nd:YAG (yttrium aluminum garnet) laser (Continuum Powerlite II 8000) operating at 20 Hz. The fundamental output of the Nd:YAG laser at 1064 nm was doubled to 532 nm to pump an OPO crystal to produce “signal” light in the near infrared (NIR) over the range 710–880 nm and “idler” light over 1350–2100 nm. The OPO idler light was then used to seed a four-crystal OPA system pumped by the Nd:YAG fundamental to produce amplified OPA signal light over the range 1350–2100 nm and OPA idler light over the range 2100–5000 nm. The vacuum wavelengths of the NIR light and both the Nd:YAG fundamental and the doubled output were measured with a pulsed wave meter (High Finesse WS6–600) that could operate over the range 350–1120 nm. The photon energy of the OPA signal light ( $E_S$ ) was calculated based on conservation of energy by subtracting the measured NIR photon energy ( $E_{\text{NIR}}$ ) from the measured doubled Nd:YAG photon energy ( $E_D = 2329.54$  meV):

$$E_S = E_D - E_{\text{NIR}}. \quad (1)$$

The photon energy of the OPA idler light ( $E_I$ ) was then determined by subtracting the OPA signal photon energy from the measured Nd:YAG fundamental photon energy ( $E_F = 1164.77$  meV):

$$E_I = E_F - E_S. \quad (2)$$

In the present experiments, the OPA idler was used to measure the three lowest energy thresholds and the OPA signal was used for the two higher energy thresholds (see Table I). The effective full bandwidth of the light was  $\sim 0.07$  meV.

A combination of optical alignment and filtering was used to separate the three beams produced by the OPO and the OPA. The selected linearly polarized light entered and exited the interaction chamber through sapphire windows, which were mounted at an angle of  $33^\circ$  to eliminate possible etaloning. The laser pulse energy was measured with a pyroelectric

TABLE I. Measured threshold energies for photodetachment from  $\text{In}^- (^3P_J)$  to  $\text{In} (^2P_J)$  obtained from fits of the  $s$ -wave Wigner law [Eq. (3)] to the measured data.

Threshold	Energy $E_t$ (meV)
$^3P_1 \rightarrow ^2P_{1/2}$	307.86(6)
$^3P_0 \rightarrow ^2P_{1/2}$	383.92(6)
$^3P_2 \rightarrow ^2P_{3/2}$	487.6(6)
$^3P_1 \rightarrow ^2P_{3/2}$	582.0(3)
$^3P_0 \rightarrow ^2P_{3/2}$	658.4(9)

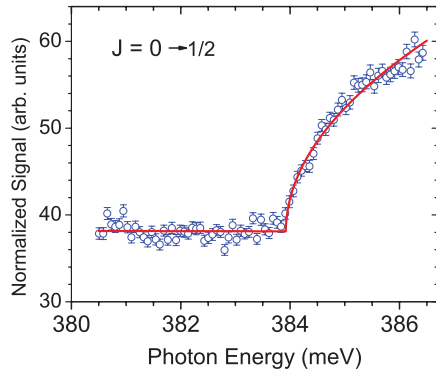


FIG. 2. (Color online) A fit of the  $s$ -wave Wigner law [Eq. (3)] (solid line) to the measured relative photodetachment cross-section data (circles) near the threshold for the  $\text{In}^- (^3P_0)$ -to- $\text{In} (^2P_{1/2})$  ground-state-to-ground-state transition. The energy at the threshold corresponds to the electron affinity of In.

detector (Ophir PE9) placed immediately outside the vacuum exit window. The energy per laser pulse through the interaction region was typically in the range 0.05–0.2 mJ with a pulse duration of 5–7 ns. To reduce room air water vapor absorption by strong  $\text{H}_2\text{O}$  bands over the photon energy ranges 420–500 and 630–690 meV (HITRAN 2008 database [23]), a tube flushed with dry nitrogen gas was used to enclose the laser beam path for  $\sim 80\%$  of the 2.5-m path from the OPO-OPA to the vacuum chamber entrance window.

The performance of the experimental system was verified by performing threshold photodetachment spectroscopy of aluminum negative ions using OPA idler light near 2900 nm. The threshold for the  $\text{Al}^- (3p^2\ ^3P_2)$  to  $\text{Al}(3p\ ^2P_{1/2})$  transition was measured to be 424.36(4) meV, which is in excellent agreement with the more precise accepted value of 424.348(25) meV measured by Scheer *et al.* [3]. In addition, the wave-meter calibration was verified by measuring the wavelength of a stabilized helium-neon laser.

The measured relative photodetachment cross sections near the thresholds for detachment from the  $\text{In}^- J = 0$  and 1 states to the  $\text{In} J = 1/2$  ground state are shown in Figs. 2 and 3, respectively. The photon energy bin width chosen for these figures was 0.074 meV, which is comparable to the laser bandwidth. The baseline signal below the threshold energy

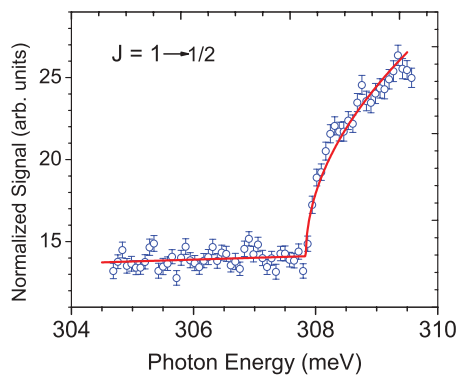


FIG. 3. (Color online) A fit of the  $s$ -wave Wigner law [Eq. (3)] (solid line) to the data (circles) near the  $\text{In}^- (^3P_1)$ -to- $\text{In} (^2P_{1/2})$  threshold.

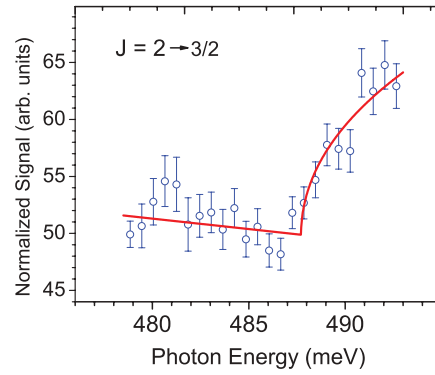


FIG. 4. (Color online) A fit of the  $s$ -wave Wigner law [Eq. (3)] (solid line) to the data (circles) near the  $\text{In}^- (^3P_2)$ -to- $\text{In} (^2P_{3/2})$  threshold.

for  $J = 0$  (Fig. 2) is due to photodetachment from ions in the excited fine-structure states ( $J = 1$  and 2) that detach at lower photon energies; similarly, the baseline below the  $J = 1$  threshold (Fig. 3) is due to detachment from ions in the  $J = 2$  state and possible weakly bound metastable state ions in the beam. It was not possible to operate the OPA at photon energies low enough to reach the threshold for detachment from the  $\text{In}^- J = 2$  state to the  $\text{In} J = 1/2$  ground state at 213.3 meV (5813 nm). However, the threshold for detachment from  $\text{In}^- J = 2$  to the  $\text{In} J = 3/2$  excited state was observed (see Fig. 4). The bin width for Fig. 4 was chosen to be a wider value (0.6 meV) to improve the statistics for presentation purposes. In addition, weak thresholds were observed for transitions from the  $\text{In}^- J = 0$  and 1 states to the  $\text{In} J = 3/2$  state.

For a limited range above an opening threshold, the photodetachment cross section is based on the Wigner threshold law [24]:

$$\sigma = (\sigma_0 + mE) + a(E - E_t)^{\ell+1/2}, \quad (3)$$

where  $E$  is the photon energy,  $E_t$  is the threshold energy,  $\ell$  is the orbital angular momentum of the departing electron, and  $a$  is a scaling constant. The background cross section due to photodetachment to lower energy thresholds is represented in the present case by the linear term  $(\sigma_0 + mE)$ , which is assumed to have constant values for the intercept  $\sigma_0$  and slope  $m$  over the narrow energy range used to fit the near-threshold data. In the present experiments, a  $p$  electron is detached from the  $\text{In}^-$  ion, thus the angular momentum selection rule  $\Delta\ell = \pm 1$  dictates that the departing electron will be either  $s$  or  $d$ . Near threshold, the  $s$  wave ( $\ell = 0$ ) will dominate, and only this term was included in the fits of the Wigner law used to extract threshold energies in the present analysis.

The measured threshold energies for the observed transitions are listed in Table I. The quoted  $1\sigma$  uncertainties include statistical uncertainties associated with the fits, photon energy calibration and bandwidth uncertainties and possible Doppler shifts due to relative beam angles. The uncertainties are substantially greater for transitions to the  $\text{In} J = 3/2$  excited state because of the larger relative backgrounds due to the open continuum channels. Photodetachment cross-section measurements were taken over larger photon energy ranges than shown in Figs. 2–4, and the low- and high-energy ends

were successively trimmed to narrow the range of the fit near threshold to determine the range of validity of the Wigner law in this case. The Wigner law [Eq. (3)] was found to be valid up to several meVs above threshold for the transitions in the present study. In addition, fits were performed with the background held constant for very narrow ranges near threshold, rather than the linear background form used for wider range fits, and the fitted threshold values were the same within uncertainty. The data were also analyzed using a range of photon energy bin widths from 0.3 to 3 times the laser bandwidth, and the fitted threshold values were found to be independent of the chosen bin width over this range. Detailed comparison of the relative strengths of the observed transitions was precluded by differences in the optical setup between measurements taken over the large photon energy range of this study; however, it appears that the transitions from the  $\text{In}^- J = 0$  ground state are relatively stronger than would be predicted by statistical population of the ionic levels [25]. This observation is not surprising given the substantial fine-structure splittings in the negative ion, resulting in much stronger binding for the  $J = 0$  ground state.

The results for the electron affinity of In and the fine-structure intervals of  $\text{In}^-$  are summarized in Table II, together with comparisons to previous values. The measured threshold for the  $\text{In}^- (5p^2\ ^3P_0)$ -to- $\text{In} (5p^2\ ^2P_{1/2})$  ground-state-to-ground-state transition determines the electron affinity of In to be 383.92(6) meV. The  $\text{In}^- J = 0-1$  fine-structure interval was determined by subtracting the threshold for  $^3P_1 \rightarrow ^2P_{1/2}$  from the threshold for  $^3P_0 \rightarrow ^2P_{1/2}$ . The  $\text{In}^- J = 0-2$  fine-structure interval was determined by subtracting the threshold for  $^3P_2 \rightarrow ^2P_{3/2}$  from the threshold for  $^3P_0 \rightarrow ^2P_{1/2}$ , then subtracting the well-known  $\text{In} J = 1/2-3/2$  splitting energy of 274.3272 meV [13]. The fine-structure intervals of  $\text{In}^-$  were determined to be 76.06(7) meV for  $J = 0-1$  and 170.6(6) meV for  $J = 0-2$  [and 94.5(6) meV for  $J = 1-2$ ].

The binding energies of the  $\text{In}^- J = 0$  and 1 states were further confirmed by measuring the thresholds for transitions from those states to the  $\text{In} J = 3/2$  excited state (see Table I). Subtracting the  $\text{In} J = 1/2-3/2$  interval (274.3272 meV [13])

from the measured thresholds yields the binding energies to be 384.1(9) meV for  $\text{In}^- J = 0$  and 307.7(3) meV for  $\text{In}^- J = 1$ ; both of these values agree within uncertainty with the more precise values from the ground state  $\text{In} J = 1/2$  thresholds of 383.92(6) and 307.86(6) meV, respectively.

The present result for the electron affinity of In, 383.92(6) meV, is significantly different from the previous measurement of 404(9) meV by Williams *et al.* [15]. However, the present fine-structure intervals of 76.06(7) meV for  $J = 0-1$  and 170.6(6) meV for  $J = 0-2$  are in excellent agreement with their measurements of 76(9) and 175(9) meV, respectively [15]. Williams *et al.* used the technique of laser photodetachment electron spectroscopy, in which the kinetic energies of the ejected electrons were measured following photodetachment with a fixed frequency laser. This technique is very good for obtaining exploratory information about a negative ion, however, the resolution is limited to meVs, and calibration of the absolute kinetic energy scale for the photoelectrons is a substantial challenge [1,9,10]. In contrast, the laser photodetachment threshold spectroscopy technique used in the present study permits measurements of a much higher accuracy and precision, since it relies on the straightforward measurement of laser wavelengths to set the energy scale. The challenges of calibrating the absolute energy for the photoelectron spectroscopy technique may explain the discrepancy between the previous results [15] and the present results; note that whereas the absolute binding energy for the  $\text{In}^- ^3P_0$  ground state reported by Williams *et al.* [15] differs from our value by 20 meV, their *relative* binding energies for the  $J = 0, 1,$  and  $2$  fine-structure levels agree with our values to better than 5 meV, which is well within the quoted uncertainties. Furthermore, the high resolution of threshold spectroscopy used in the present experiment permitted a reduction in the uncertainties from the previous measurements [15] for the electron affinity of In by a factor of 150 and for the fine-structure intervals of  $\text{In}^-$  by factors of 130 for  $J = 0-1$  and 15 for  $J = 0-2$ .

The present value for electron affinity is in good agreement with a substantial number of previous theoretical calculations

TABLE II. Comparison of the present results for the electron affinity of In and fine-structure intervals of  $\text{In}^-$  to previous measurements and theoretical calculations. All values are meVs. LPTS, laser photodetachment threshold spectroscopy; LPES, laser photodetachment electron spectroscopy; LSD-GX, local spin density functional; CIPSI, multireference configuration interaction; MCDF, multiconfiguration Dirac-Fock; RCC, relativistic coupled cluster; MCHF-CCSD, multiconfiguration Hartree-Fock with coupled cluster; IHFSCC, intermediate-Hamiltonian Fock-space coupled cluster.

Study	Method	Electron affinity	$J = 0-1$	$J = 0-2$
Experiment				
Present	LPTS	383.92(6)	76.06(7)	170.6(6)
Williams <i>et al.</i> [15]	LPES	404(9)	76(9)	175(9)
Theory				
Guo <i>et al.</i> [16]	LSD-GX	371		
Arnau <i>et al.</i> [17]	CIPSI	380		
Wijesundera [18]	MCDF	393		
Eliav <i>et al.</i> [19]	RCC	419		
Sundholm <i>et al.</i> [20]	MCHF-CCSD	374(15)		
Figgen <i>et al.</i> [21]	IHFSCC	403		

(see Table II). The theoretical results of Arnau *et al.* [17], Wijesundera [18], and Sundholm *et al.* [20] are particularly close to the present value, each being within 10 meV. Most of the theoretical studies did not indicate uncertainties, however, Sundholm *et al.* [20] estimated an uncertainty of 15 meV in their calculated electron affinity. That study used large-scale multiconfiguration Hartree-Fock calculations to obtain valence limits for the electron affinity, then estimated core-correlation contributions using coupled cluster calculations with relativistic corrections. Their final value for the In electron affinity, 374(15) meV [20], differs from the present value by less than their estimated uncertainty. Sundholm *et al.* [20] further observed that, with their method, “the calculated electron affinities are usually somewhat smaller than the measured ones;” that observation is confirmed by the high accuracy of the present results.

In summary, we have measured the electron affinity of In and the fine-structure intervals of  $\text{In}^-$  with sub-meV uncertainty. Our result for the electron affinity of 383.92(6) meV substantially revises the previous measurement of 404(9) meV [15]. The uncertainty of the previous experimental value (9 meV) [15] is of the same order of magnitude as the spread of the existing theoretical values, which range from

371 to 419 meV [16–21]. Our present measurement of the electron affinity yields an uncertainty (0.06 meV) that is two orders of magnitude smaller than the uncertainty of the earlier measurement, thus providing an excellent test case for state-of-the-art atomic structure theory that incorporates detailed analysis of correlation for both the valence and core electrons. Overall for group III elements, there appears to be good agreement between experiment and theory for the electron affinities of all members except Ga [10]. Significant discrepancies remain between the measured value for the electron affinity of Ga (430(30) meV [26,27]) and the calculated theoretical values (e.g., 297(13) meV [20]). We plan to perform a similar study of  $\text{Ga}^-$  using infrared laser photodetachment threshold spectroscopy to measure precise values for the binding energies of the negative ion to help resolve this discrepancy.

We thank E. Eliav for helpful correspondence and Ken Bixler for technical assistance. This material is based in part upon work supported by National Science Foundation under Grant No. 0757976. D.J.C., Y.-G.L., and D.J.M. received partial support from Denison University’s Anderson Summer Research Fund.

- 
- [1] D. J. Pegg, *Rep. Prog. Phys.* **67**, 857 (2004).
- [2] M. Scheer, R. C. Bilodeau, and H. K. Haugen, *Phys. Rev. Lett.* **80**, 2562 (1998).
- [3] M. Scheer, R. C. Bilodeau, J. Thogersen, and H. K. Haugen, *Phys. Rev. A* **57**, R1493 (1998).
- [4] R. C. Bilodeau and H. K. Haugen, *Phys. Rev. Lett.* **85**, 534 (2000).
- [5] P. Andersson, A. O. Lindahl, C. Alfredsson, L. Rogstrom, C. Diehl, D. J. Pegg, and D. Hanstorp, *J. Phys. B* **40**, 4097 (2007).
- [6] P. Andersson, A. O. Lindahl, D. Hanstorp, and D. J. Pegg, *Phys. Rev. A* **79**, 022502 (2009).
- [7] C. W. Walter, N. D. Gibson, C. M. Janczak, K. A. Starr, A. P. Snedden, R. L. Field III, and P. Andersson, *Phys. Rev. A* **76**, 052702 (2007).
- [8] C. W. Walter, N. D. Gibson, R. L. Field III, A. P. Snedden, J. Z. Shapiro, C. M. Janczak, and D. Hanstorp, *Phys. Rev. A* **80**, 014501 (2009).
- [9] T. Andersen, H. K. Haugen, and H. Hotop, *J. Phys. Chem. Ref. Data* **28**, 1511 (1999).
- [10] T. Andersen, *Phys. Rep.* **394**, 157 (2004).
- [11] *CRC Handbook of Chemistry and Physics*, 90th Edition, edited by D. R. Lide (CRC Press, Boca Raton, FL, 2009).
- [12]  $\text{In}^-$  and several other group III ions were photodetached using a conventional broadband light source by D. Feldmann, R. Rackwitz, E. Heinicke, and H. J. Kaiser, *Z. Naturforsch* **32**, 302 (1977), however, the light source could not be operated at a wavelength long enough to reach the threshold to obtain the electron affinity or fine-structure intervals.
- [13] C. E. Moore, *Atomic Energy Levels Vol. III*, Natl. Bur. Stand. (US) Circ. No. 467 (US Government Printing Office, Washington, DC, 1952).
- [14] P. J. Mohr, B. N. Taylor, and D. B. Newell, *J. Phys. Chem. Ref. Data* **37**, 1187 (2008).
- [15] W. W. Williams, D. L. Carpenter, A. M. Covington, J. S. Thompson, T. J. Kvale, and D. G. Seely, *Phys. Rev. A* **58**, 3582 (1998).
- [16] Y. Guo and M. A. Whitehead, *Phys. Rev. A* **38**, 3166 (1988).
- [17] F. Arnau, F. Mota, and J. J. Novoa, *Chem. Phys.* **166**, 77 (1992).
- [18] W. P. Wijesundera, *Phys. Rev. A* **55**, 1785 (1997).
- [19] E. Eliav, Y. Ishikawa, P. Pyykko, and U. Kaldor, *Phys. Rev. A* **56**, 4532 (1997).
- [20] D. Sundholm, M. Tokman, P. Pyykkot, E. Eliav, and U. Kaldor, *J. Phys. B* **32**, 5853 (1999).
- [21] D. Figgen, A. Wedig, H. Stoll, M. Dolg, E. Eliav, and U. Kaldor, *J. Chem. Phys.* **128**, 024106 (2008).
- [22] E. Eliav (private communication).
- [23] L. S. Rothman, *J. Quant. Spectrosc. Radiat. Transfer* **110**, 533 (2009).
- [24] E. P. Wigner, *Phys. Rev.* **73**, 1002 (1948).
- [25] P. C. Engelking and W. C. Lineberger, *Phys. Rev. A* **19**, 149 (1979).
- [26] W. W. Williams, D. L. Carpenter, A. M. Covington, M. C. Koepnick, D. Calabrese, and J. S. Thompson, *J. Phys. B* **31**, L341 (1998).
- [27] A reanalysis of the data in Ref. [26] by H. Hotop (unpublished; cited in Ref. 9) accounting for the effects of fine structure yielded a value of 410(40) meV for the electron affinity of Ga.